Modeling of a Continuous Rotating Disk Polycondensation Reactor for the Synthesis of Thermoplastic Polyesters

SEONG ILL CHEONG* and KYU YONG CHOI†

Department of Chemical Engineering, University of Maryland, College Park, Maryland 20742

SYNOPSIS

A dynamic multicompartment model is proposed for a continuous flow rotating disk reactor for the finishing stage melt polycondensation of poly(ethylene terephthalate). In the multicompartment reactor model, ethylene glycol is removed from both the bulk melt phase and the film phase formed on the rotating disks. The specific interfacial area for the film phase is estimated using the empirical correlation for polymer film thickness, and the mass transfer coefficient is calculated using the penetration theory. The mass transfer enhancement factor is introduced to account for the increased interfacial area due to ethylene glycol bubbles. The effects of reactor design and operating parameters on molecular weight and ethylene glycol removal have been investigated through model simulations. In particular, a detailed analysis is presented on the ethylene glycol removal rate from the two phases. © 1996 John Wiley & Sons, Inc.

INTRODUCTION

Many industrially important engineering thermoplastic polymers are manufactured by multistage melt polycondensation processes using either semibatch or continuous reactors. In a continuous melt polycondensation process for poly(ethylene terephthalate) (PET), monomers (bishydroxy ethyl terephthalate) are produced first in the transesterification stage using dimethyl terephthalate or terephthalic acid as a starting material. Then they are polymerized to low-molecular-weight prepolymers in a series of stirred tank reactors at about 260 ~ 280°C and 10 ~ 30 mmHg. The polymer molecular weight is further increased at much lower pressure (0.1 ~ 1.0 mmHg) in a finishing polymerization reactor designed to handle high-viscosity polymer melt. Due to the multistage nature of this process, the final polymer properties (e.g., molecular weight, concentrations of side products) are influenced by many different factors in each stage. Often, it is difficult to monitor in each stage the progress of reaction

and the polymer properties online. If undesired deviations in the final product properties from their target values occur, it is not easy to identify the causes for such deviations and to correct them. Thus, a mathematical process model can be used as a useful tool to develop a better understanding of polymerization phenomena.

According to elementary linear polycondensation kinetics, the conversion of reactive end groups must be over 99% to obtain a degree of polymerization larger than 100. However, due to high melt viscosity in the melt polycondensation of PET, achieving such high conversion is often difficult. To increase the polymer molecular weight in the finishing polycondensation stage where reversible esterification reaction occurs, volatile condensation byproducts [e.g., ethylene glycol (EG)] must be removed effectively from the polymer melt. It is also desirable to obtain narrow molecular weight distribution to minimize the production of low-molecular-weight polymers. Thus, the design and operation of a finishing stage polycondensation reactor are focused on devising the means for effective removal of volatile compounds.

The finishing polymerization reactors that are used in industry include rotating disk reactors or similar type (e.g., twin-shaft disk reactor), wiped film reactors, screw reactors, and cage reactors. Many

different types of finishing polycondensation reactor configurations are reported in patent literature. From the process modeling point of view, developing a model of a reactor with complex geometry, such as a finishing polycondensation reactor, is a challenging task. Polymerization kinetics are not always perfectly understood (qualitatively and quantitatively), and obtaining the numerical values of model parameters (kinetic parameters and reactor specific parameters) is a problem. Thus, if one wants to develop a reasonable reactor model capable of predicting the overall reactor behavior and resulting polymer properties, it may be necessary to make appropriate assumptions and model simplifications.

In this work, a continuous flow rotating disk reactor is modeled. The rotating disk reactor is a horizontal cylindrical vessel with a horizontal rotating shaft on which disks are mounted. These disks are immersed partially in the bulk liquid. Low-molecular-weight prepolymers are continuously supplied to the reactor. As the shaft rotates at relatively low speed, polymer melt is partially dragged upward onto the disks and thin layers or films of polymer melt are formed on the disk surfaces. High vacuum is applied to remove volatile species (most importantly, ethylene glycol) from these thin polymer melt films. For calculation of the amount of ethylene glycol removed from the polymer melt, we need to know the polymer holdup on the disks and the effects of reactor operating conditions on the rate of ethylene glycol removal and polymer molecular weight. One main reason for choosing this reactor configuration in this work is that the reactor geometry is well defined and thus the reactor modeling is more tractable. With some modifications, the method used in modeling the rotating disk reactor can be applied to more complex reactor systems.

In our previous work,[1,2] we investigated the polymer melt film forming phenomena on a rotating disk and the melt polycondensation of PET in a semibatch rotating disk reactor for various reactor operating conditions. Experimental measurements of polymer layer thickness were made and it was found that the layer thickness varies along the disk radius. The measured polymer melt layer thickness data were used to develop an empirical correlation to calculate the layer thickness and polymer holdup. A bench scale laboratory semibatch rotating disk reactor was designed and used to investigate mass transfer and reaction phenomena. A two-parameter model was also proposed for a semibatch reactor in which the mass transfer and reaction in a film phase and a bulk melt phase were treated separately. The mass transfer interfacial area was calculated from

the experimental data, and the model predictions were compared with experimental data. In this article we extend the rotating disk reactor model to a continuous polycondensation reactor system and present a multicompartment model for the finishing stage of PET polycondensation.

In a continuous rotating disk reactor, polymer melt travels at relatively low speed toward the reactor outlet and polymer molecular weight increases in the axial direction. High vacuum is applied to remove ethylene glycol and other small amounts of volatile species (e.g., water, acetaldehyde). In industrial polycondensation processes, it is desired to minimize any effects, such as axial dispersion or backmixing, that can cause the deviation from the plug flow and result in the broadening of molecular weight distribution or the formation of polymer gels or low-molecular-weight oligomers. In industrial PET reactors, a stagnant zone may develop near the outlet of the reactor. The polymers that have excessively and undesirably long residence time in the reactor at high reaction temperature may cause some problems. Although it has not been verified unambiguously, it is widely speculated by practicing reactor engineers that the presence of low-molecular-weight polymers in the final polyester product may be due to some degradation of high-molecular-weight polymers that stay too long in the reactor, probably in stagnant zones. If such low-molecular-weight polymers are present, the quality of polyester films or fibers deteriorates and such products will be rejected by end users.

Recently, there have been a few reports on the modeling and analysis of continuous finishing stage polycondensation reactors for the synthesis of PET.[3-9] Notably, Ravindranath and Mashelkar[4,5] modeled a wiped film reactor and a rotating disk type reactor. Similar modeling works have also been reported by Kumar and co-workers[6,7] and by Amon and Denson.[10] Although few experimental data were used or presented, these works provide an excellent analysis of the finishing stage polycondensation processes through a parameter sensitivity study. Recently, we proposed a two-phase model[8,9] in which the entire reactor is viewed as a composite of two phases (i.e., polymer melt phase and vapor phase). The polymer melt phase includes both the bulk and the film phases. A single effective mass transfer parameter is used to account for the rate of mass transfer of volatile species from the polymer phase to the vapor phase. Although the two-phase model has its major advantage in that the model is independent of specific reactor geometry because a single adjustable parameter is used for mass transfer, this

advantage can also be considered as a drawback of the model. This is because the two-phase model is not capable of analyzing the effect of specific reactor design and operating parameters such as the number of disks and disk rotating speed. Thus, a new modeling approach is needed to quantify explicitly the effect of reactor design and operating parameters on the reactor performance. In this work the multicompartment model is developed to describe the behavior of a continuous flow finishing polycondensation reactor. Through dynamic model simulations, we shall analyze the effect of various reactor design and operating variables on the reactor performance and polymer molecular weight.

FLOW CHARACTERIZATION

In the continuous rotating disk reactor to be modeled in this work, multiple disks are mounted on a central horizontal shaft. The disks are immersed partially (about 50%) in the liquid phase. As the shaft turns, a small amount of liquid is dragged upward onto a rotating disk, forming a thin liquid film. After a short exposure to vapor phase, the polymer film is then mixed with the bulk liquid as the disk edge enters the bulk liquid phase. There is also a continuous flow of liquid in the axial direction. The reactor is then divided into a finite number of equal-sized virtual compartments. Each compartment has a disk, bulk liquid phase, and a film phase. To justify the proposed multicompartment model structure, we carried out bench scale experiments using a model fluid and a model reactor at ambient temperature and pressure. Since inert tracer material is used, no mass transfer or reaction occurs during the experiment. The flow characteristics of PET melt in a real reactor may not be identical with those observed in the model experimental system because the polymer holdup on the disks changes as polymer molecular weight changes in the reactor. The viscosity of polymer melt is also higher than the viscosities of the model fluid used in our flow characterization experiments. However, it is very difficult to conduct a flow test in a real continuous flow melt polycondensation reactor. Therefore, the flow characterization test with the model fluid will only give an approximate measure of the flow patterns in a real polymerization reactor system.

In a model continuous flow rotating disk (reactor) system where no reaction occurs, the fluid moves in a transversal direction and some fluids are dragged upward onto the disks by the shaft rotation. Let us consider the jth compartment (c.f. Fig. 4). The

tracer concentration in the liquid film at the inlet of the jth compartment is given by

$$C_{j,f} = C_{j,b}(t - t_f) \qquad (1)$$

where $C_{j,b}$ is the tracer concentration in the bulk phase of the jth compartment and t_f is the time for the film phase exposed to the vapor phase. In this model system, tracer material is not removed from the film and bulk phases. In the bulk liquid phase, the tracer concentration in the jth compartment is calculated by solving the following mass balance equation:

$$V_b \frac{dC_{j,b}}{dt} = q(C_{j-1,b} - C_{j,b}) + \frac{V_f}{t_f}(C_{j,f} - C_{j,b}) \qquad (2)$$

To test the applicability of the multicompartment model, a bench scale experiment has been carried out. Figure 1 shows a schematic diagram of the experimental apparatus. The test vessel, which represents a finishing stage polycondensation reactor, is a horizontal cylindrical vessel of 35 cm long with a central shaft to which 10 disks ($D = 9.5$ cm) are mounted. An aqueous solution of carboxy methyl cellulose (CMC) is fed to the vessel. The steady state flow rate of the CMC solution is maintained while a disk assembly is rotated at a prespecified speed. A tracer solution is prepared by adding a predeter-
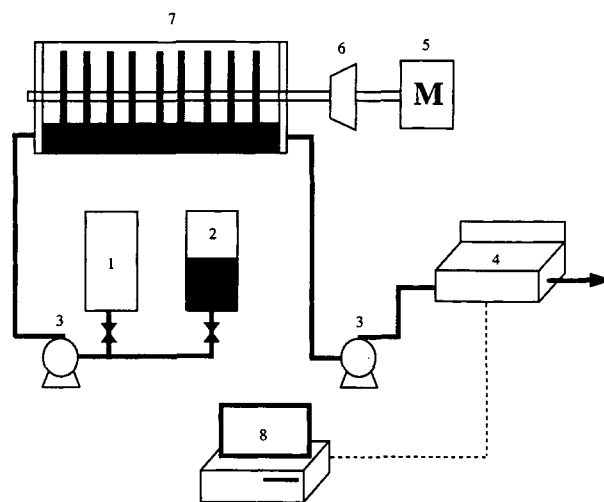
1. Fresh aqueous CMC solution	2. Dye aqueous solution
3. Micro pump	4. Spectrophotometer
5. Variable speed motor	6. Motor speed reducer
7. Plexiglass rotating disk reactor	8. Data acquisition computer

Figure 1   An experimental setup for flow characterization experiments.
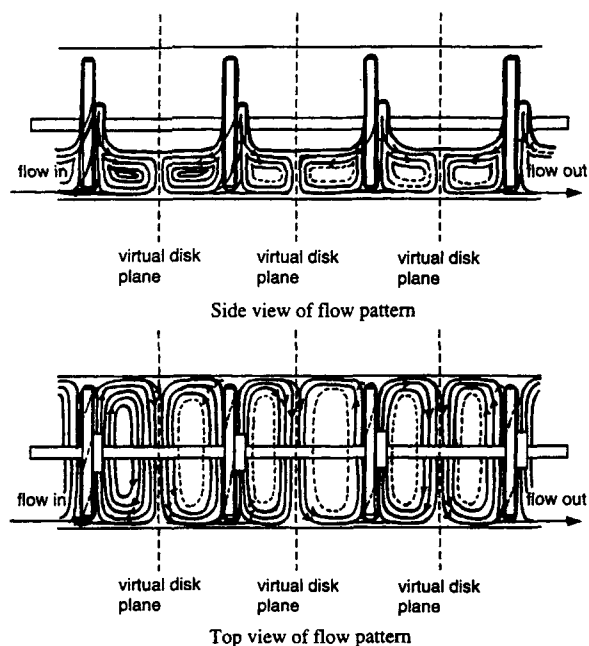
Figure 2   Stream lines in a continuous rotating disk reactor with CMC solution.

mined amount of methylene blue to the CMC solution. The tracer solution is then stored in a separate storage tank. To avoid any degradation of the CMC solution, it was prepared before each experiment. The flow test was started by injecting the tracer solution as a step function. The concentration of tracer at the vessel outlet was measured continuously by a spectrophotometer interfaced with a data acquisition computer. The linearity of the light absorbance with the tracer concentration was first confirmed and used for calibration.

Figure 2 illustrates the top and side views of a typical streamlined development observed in the experiments. In each diagram, dashed lines indicate the virtual disk planes which lie midway between the two neighboring disks that are equally spaced. It is along these virtual disk planes, as well as the disks themselves, that most of the through-flow occurs. It is seen that a characteristic S pattern emerges. In addition, as indicated in the top view, stagnant zones are present on the lee side of each disk. The flow tests were carried out for different liquid flow rates, numbers of disks, liquid viscosity, and disk rotational speed. Figure 3 illustrates the resulting outlet tracer concentration profiles with two CMC solutions of different viscosity (20 and 60 poise) at 10 rpm. The solid lines represent the model predictions. Some discrepancies exist, but overall the multicompartment model gives a reasonable agreement with the data.

REACTOR MODEL

To develop a dynamic multicompartment model for a continuous finishing polycondensation reactor, the following polycondensation reaction is considered for a PET system:

$$E_g + E_g \underset{k'}{\overset{k}{\rightleftharpoons}} Z + EG \qquad (3)$$
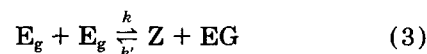
where E_g = hydroxy ethyl group, Z = diester group, and EG = ethylene glycol. The reaction rate is given by

$$r = k[E_g]^2 - 4k'[Z][EG] \qquad (4)$$

Now let us consider a continuous rotating disk reactor. As the central shaft rotates, a small amount of polymer melt is dragged upward from the bulk phase, forming a thin polymer melt layer on the surface of each disk. The polymer layer or film is then mixed again with the bulk polymer melt in the trough as the disk rotates. Volatiles such as ethylene
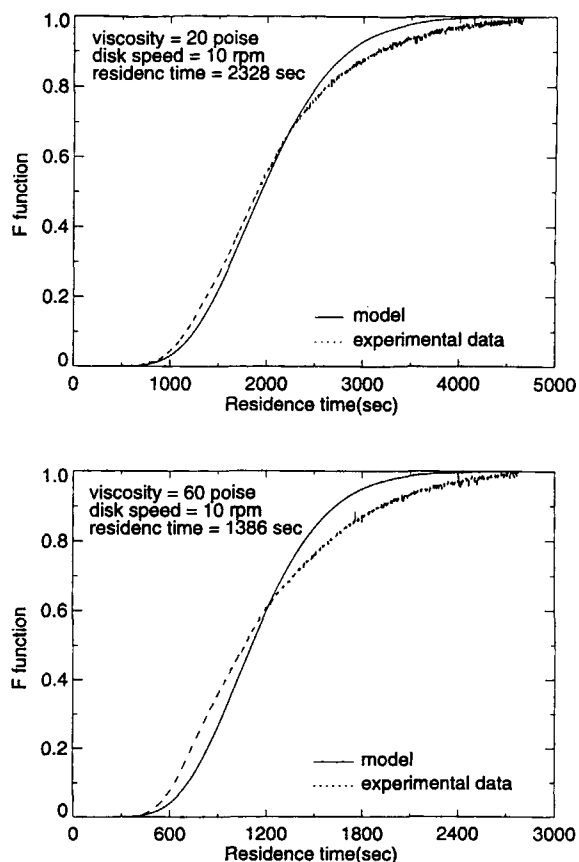

Figure 3   Exit concentration of tracer in a rotating disk reactor.
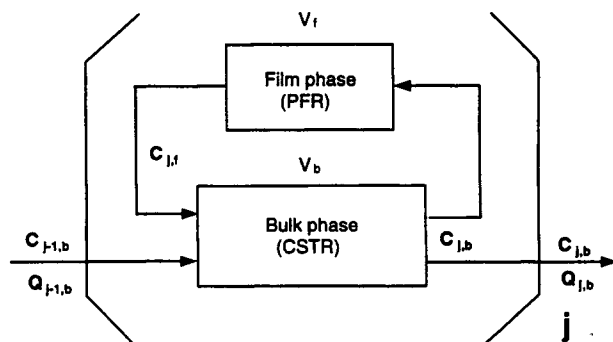
Figure 4 Multicompartment model for a continuous flow rotating disk reactor.

glycol are removed from the thin polymer layer as it is exposed to the vapor phase. The bulk polymer melt flows in a transversal direction. Volatile compounds are also removed from the bulk phase through the free surface or as tiny bubbles. To model this reactor system, we propose a multicompartment model, as illustrated schematically in Figure 4. Here the reactor is equipped with N equal-sized disks that divide the whole reactor into N equal-sized virtual compartments. Each compartment contains a disk and consists of a vapor phase, a film phase on the disk, and a bulk phase in which a disk is partially immersed. We assume that the bulk phase behavior is modeled as a continuous stirred tank reactor (CSTR) whereas the film phase is modeled as a plug flow reactor. No gravity effect is assumed for the film phase on rotating disk surfaces. In practice, there is a possibility that the polymer layers on the disks may not be mixed perfectly with the bulk phase as the disk rotates. However, in our modeling we assume that the polymers on the disk are completely mixed with the bulk phase while the disk is immersed and rotating in the bulk phase.

As the polymerization takes place in both the bulk phase and the film phase, the total interfacial area and the mass transfer coefficient must be known or estimated to calculate the ethylene glycol removal rate from the reactor. In the proposed multicompartment model, the main idea is to use the mass transfer coefficient (k_L) and specific interfacial area (a) estimated or measured separately. In the two-phase model we presented earlier,[8,9] the overall mass transfer parameter ($k_L a$) is used as a single adjustable parameter and no a priori estimation of the parameter is possible. Thus, it is not possible to quantify the effects of reactor design and operating parameters that influence the interfacial area for mass transfer. To calculate the specific interfacial area for the ro-

tating disk reactor system, the polymer holdup on each disk must be known. In ref. 1, the polymer (PET) film thickness on a rotating disk was measured and an empirical correlation was developed for the polymer holdup on a rotating disk. Ethylene glycol is removed not only from the polymer films by the diffusive mass transfer due to concentration gradient but also from the bulk melt phase, mostly in the form of small bubbles. Additional mass transfer surfaces are thus provided by these bubbles. However, it is practically difficult to estimate the number and size of bubbles and hence the interfacial area exerted by these bubbles. Thus, a combined value of mass transfer parameter for bulk phase [$(k_L a)_b$] was measured from semibatch polycondensation experiments.[2]

To account for the effect of bubbles in the film phase, we introduce an empirical parameter f (mass transfer enhancement factor). Here f is defined as the ratio of the mass transfer parameter due to bubble formation to that without bubbles in the film phase. The overall mass transfer parameter in the film phase is given as $(1 + f)(k_L a)_f$. It was shown in ref. 2 for a semibatch polycondensation system that f lies in the range of 0.5 $\sim$ 1.0 and f is only slightly affected by disk rotating speed. This implies that ethylene glycol bubbles account for about 30 $\sim$ 50% of the total mass transfer from the film phase. The effect of bubbles was indirectly accounted for in the works by some researchers. For example, Kumar et al.[7] report for a wiped film reactor system that a very high value of interfacial area is needed to obtain high molecular weight in their reaction model. The increased interfacial area may be due to the presence of ethylene glycol bubbles in real polymerization system. Amon and Denson[10] used the interfacial area for a wiped film reactor by multiplying the actual geometric surface area by an arbitrary factor of 3 to account for the presence of small ethylene glycol bubbles. The multicompartment model presented here is not also completely free of adjustable parameters because the mass transfer enhancement factor f is used; f should be determined by fitting the model with actual process data.

The mass transfer coefficient is estimated using the penetration theory and is given by $k_L = 2\sqrt{D/\pi t_f}$, where D is the diffusivity of ethylene glycol in the polymer melt ($D = 1.6 \times 10^{-4}$ cm^2/s).[11] It was observed in our semibatch polycondensation experiment and modeling studies[2] that $(k_L a)_b \ll (k_L a)_f$. In other words, the amount of ethylene glycol removed from the bulk melt phase is significantly smaller than that from the film phase. The specific

interfacial area (a) is dependent on the polymer melt holdup on the disk as well as the dimension of the disk or its wetted area. Then the modeling equations take the following form.

Bulk Phase:

$$\frac{d[E_g]_{j,b}}{dt} = -2r_{j,b} + \frac{Q_{j,b}}{V_{j,b}}([E_g]_{j-1,b} - [E_g]_{j,b})$$

$$+ \frac{V_{j,f}}{V_{j,b}t_f}([E_g]_{j,f} - [E_g]_{j,b}) \quad (5)$$

$$\frac{d[EG]_{j,b}}{dt} = r_{j,b} - (k_L a)_b([EG]_{j,b} - [EG]^*_{j,b})$$

$$+ \frac{Q_{j,b}}{V_{j,b}}([E_g]_{j-1,b} - [E_g]_{j,b})$$

$$+ \frac{V_{j,f}}{V_{j,b}t_f}([E_g]_{j,f} - [E_g]_{j,b}) \quad (6)$$

$$\frac{d[Z]_{j,b}}{dt} = r_{j,b} + \frac{Q_{j,b}}{V_{j,b}}([Z]_{j-1,b} - [Z]_{j,b})$$

$$+ \frac{V_{j,f}}{V_{j,b}t_f}([Z]_{j,f} - [Z]_{j,b}) \quad (7)$$

Film Phase:

$$v\frac{d[E_g]_{j,f}}{dx} = -2r_{j,f} \quad (8)$$

$$v\frac{d[EG]_{j,f}}{dx} = r_{j,f} - (1 + f)(k_L a)_f([EG]_{j,f} - [EG]^*_{j,f})$$

$$\quad (9)$$

$$v\frac{d[Z]_{j,f}}{dx} = r_{j,f} \quad (10)$$

The subscripts b and f represent the bulk phase and the film phase, respectively; Q is the axial flow rate, V is the volume; x is the distance for the polymer melt film on the disk to travel at speed v after the leading edge of the disk ($x = 0$) departs from the bulk phase; and t_f is the surface renewal time determined by the disk rotating speed.

The polymer melt holdup on the rotating disk surface is calculated using the following equation:

$$V_f = \int_{r_i}^{r_o} r\omega h\left(1 - \frac{\rho g h^2}{3\mu r\omega}\right) dr \quad (11)$$

where r_i is the inner radius of the wetted area, r_o the outer radius of the wetted area, ω the disk rotating speed, ρ the fluid density, and μ the viscosity.

Here the film thickness (h) is calculated using the following empirical equation for PET melt[1]:

$$\Gamma = 2.4 \times 10^{-5}\, Ca^{1.267}\, \overset{-1.362}{Re}\, Fr^{1.554}\Phi^{-2.839} \quad (12)$$

where $\Gamma = h(\rho g/\mu r\omega)^{0.5}$ (dimensionless film thickness), $Ca = \mu\omega r/\sigma$ (capillary number), $Re = \rho r^2\omega/\mu$ (Reynolds number), $Fr = r\omega^2/g$ (Froude number), $\Phi = r/R$ (dimensionless radius), r is the radial position, and R is the disk radius. Figure 5 shows the PET melt layer thickness profiles measured for three different values of X_n at 20 rpm in a batch rotating disk reactor. The experimental data were obtained for a single rotating disk at 280°C using a specially made probe to measure the film thickness at different radial positions.[1] The symbols in Figure 5 are the experimental data, and the lines are the computed values using eq. (12). It is seen that polymer
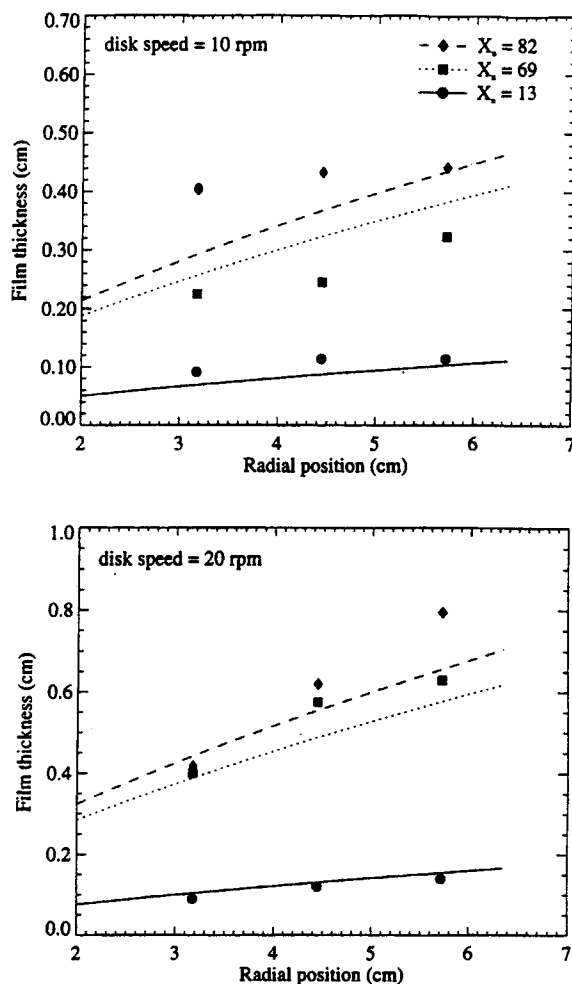

Figure 5 Polymer layer thickness profiles. Symbols: experimental data; lines: eq. (12).
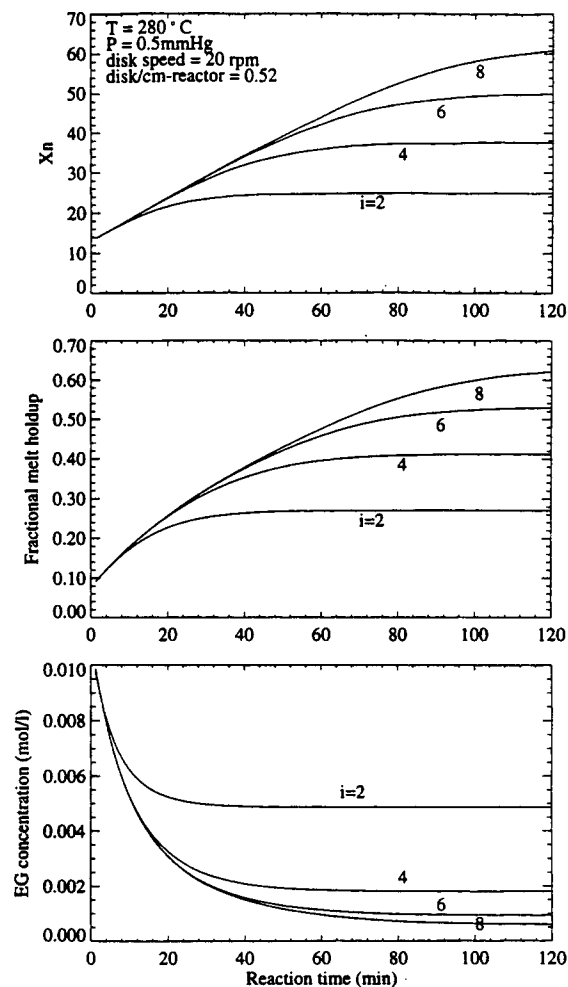
Figure 6 Degree of polymerization, fractional melt holdup, and ethylene glycol concentration in different virtual disk compartments.
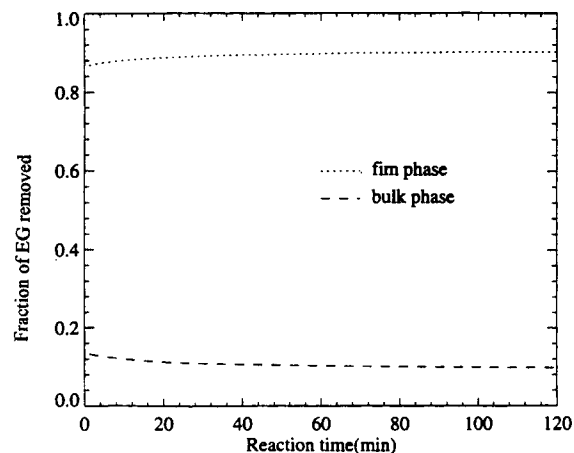

Figure 7 Fraction of ethylene glycol removed from bulk phase and film phase.

The equilibrium mole fraction of ethylene glycol at the interface is

$$X_{EG} = \frac{P}{\gamma_{EG}P^0_{EG}} \qquad (14)$$

where P is the reactor pressure and γ_{EG} is the activity coefficient which is calculated using the Flory–Huggins equation:

layer thickness increases with polymer molecular weight and the layer thickness is not quite uniform in the radial direction on the disk. In a continuous flow rotating disk reactor, the polymer molecular weight increases with the reactor length. Therefore, this figure suggests that the distance between the disks may have to be adjusted properly so that the polymer layers formed on two neighboring disks do not touch against each other.

The concentration of ethylene glycol at the vapor–liquid (melt) interface is estimated as follows. The vapor pressure of ethylene glycol is calculated using the following equation[12]:

$$\ln P^0_{EG} = 49.703 - 8.06 \times 10^3/T$$

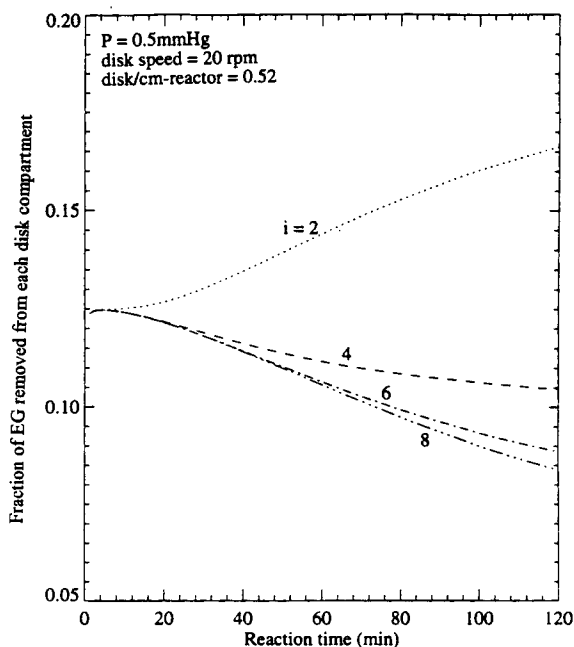$$- 4.042 \ln T (P^0_{EG} \text{ in mmHg}, T \text{ in K}) \qquad (13)$$

Figure 8 Fraction of ethylene glycol removed from each disk compartment.
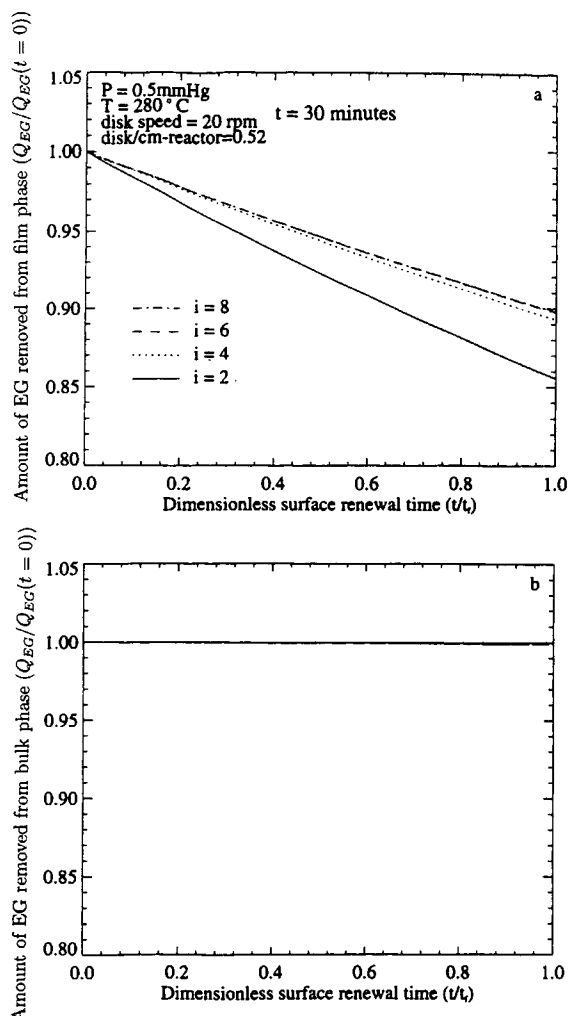
Figure 9 Amount of ethylene glycol removed from film phase and bulk melt phase during one dimensionless surface renewal time.

$$\ln \gamma_{EG} = \ln\left\{1 - \left(1 - \frac{1}{m}\right)\Psi_2\right\}$$
$$+ \left(1 - \frac{1}{m}\right)\Psi_2 + \chi\Psi_2^2 \quad (15)$$

where subscript 2 represents the polymer, Ψ_2 the volume fraction of polymer, χ (=1.3) the Flory interaction parameter, and m the ratio of molar volumes of polymer to ethylene glycol. Since the mole fraction of ethylene glycol is small, $\Psi_2 \to 1$ and eq. (15) is reduced to

$$\gamma_{EG} = \frac{1}{m}\exp\left(1 - \frac{1}{m} + \chi\right) \quad (16)$$

Then the interfacial ethylene glycol concentration is given by

$$[EG]^* = \frac{P[E_g]}{2(P_{EG}^0\gamma_{EG} - P)} \quad (17)$$

The amount of ethylene glycol removed from each compartment during the film exposure time t_f is given as

$$Q_{EG} = \int_0^{t_f} \{(1 + f)(k_La)_f([EG] - [EG]_f^*)V_f$$
$$+ (k_La)_b([EG]_b - [EG]_b^*)V_b\}dt \quad (18)$$

RESULTS AND DISCUSSION

The primary objective in operating the finishing polycondensation reactor is to obtain a desired high polymer molecular weight (or the degree of polymerization, X_n). For a given reactor geometry, the process parameters that affect the polymer molecular weight are reaction temperature, pressure, disk rotational speed, and number of disks. In the simulations to follow, we shall focus on the effects of disk-related operating and design parameters. For simulation purposes, the following reactor dimension is used as a base: reactor diameter = 14.0 cm, reactor diameter = 12.7 cm, total number of disks = 8, distance between the disks = 1.92 cm (equally spaced). The concentrations of reactive groups in the feed prepolymers are $[E_g]$ = 0.921 mol/L, [Z] = 5.528 mol/L. The mass transfer parameters used are $(k_La)_b$ = 4.2 × 10^{-3} s^{-1}, $(1 + f)(k_La)_f$ = 0.09 s^{-1} (ref. 2). For each reaction time interval (Δt), the foregoing modeling equations are solved to calculate the bulk phase concentrations of functional end groups and ethylene glycol concentration. The forward reaction rate constant used in the model calculations is k = (9.77 × 10^3 ± 33)exp[−((13.40 ± 3.785) × 10^3)/T](L/mol min) (ref. 2), and the equilibrium constant K = 0.5 is used.

The profiles of degree of polymerization, fractional melt holdup, and ethylene glycol concentration in several virtual compartments during startup operation period are shown in Figure 6. In this simulation, the mean reactor residence time is 2 h and the disk rotating speed is 20 rpm. Here i represents the disk number counted from the reactor inlet. The reactor pressure is 0.5 mmHg and temperature is 280°C. Notice that the polymer molecular weight and total melt holdup on the disk increase as the polymer melt travels through the reactor (i.e., as i
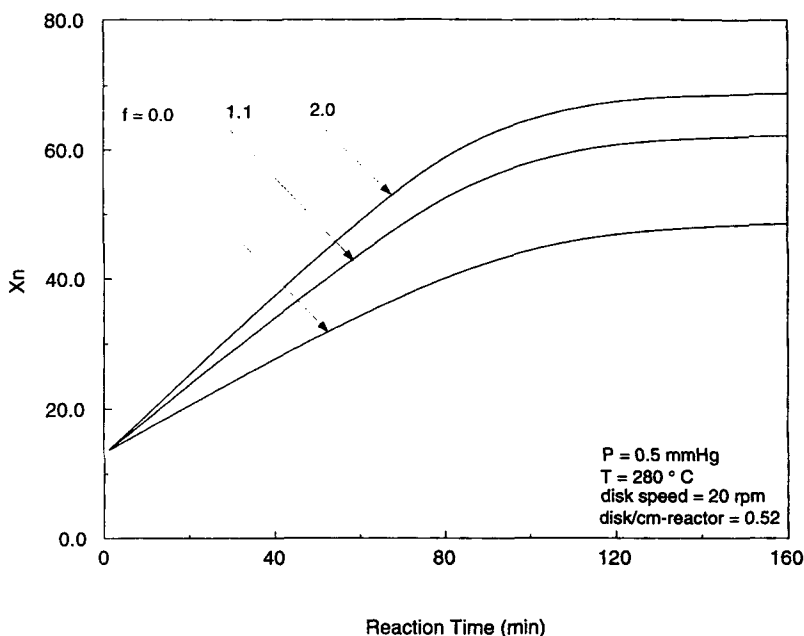
Figure 10   Effect of mass transfer enhancement factor (f).

increases). The concentration of ethylene glycol in each compartment decreases sharply as the continuous operation starts. The equilibrium ethylene glycol concentration in the compartments near the reactor inlet is much higher than those near the outlet of the reactor. The second diagram in Figure 6 also indicates that the fractional melt holdup on the disk (polymer holdup on a disk/total polymer in each compartment) in the compartments near the reactor

outlet increases to more than 60%. Large polymer holdup means smaller specific interfacial area and less effective ethylene glycol removal per revolution of the disk. Since the multicompartment model deviates from the ideal plug flow model as assumed in the two-phase model,[8,9] it takes slightly more than one residence time to reach the steady state.

It is also of interest to know how much ethylene glycol is removed from the film phase and the bulk
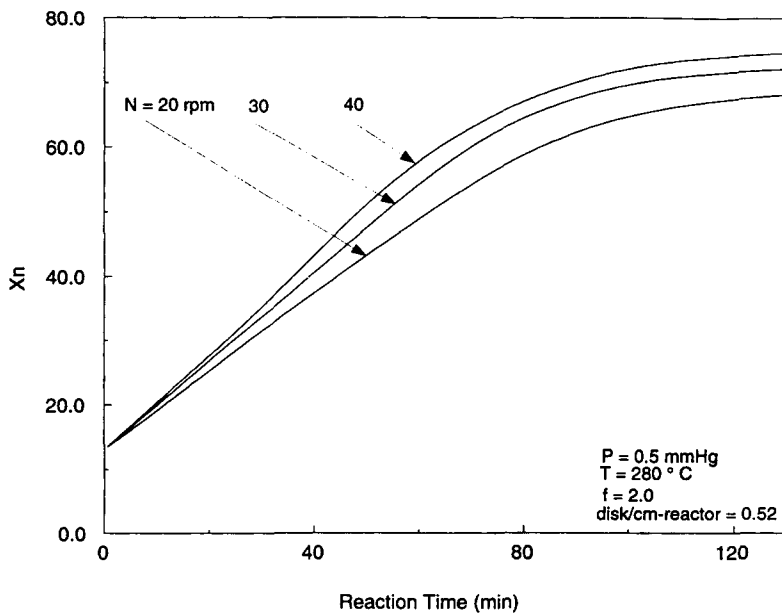

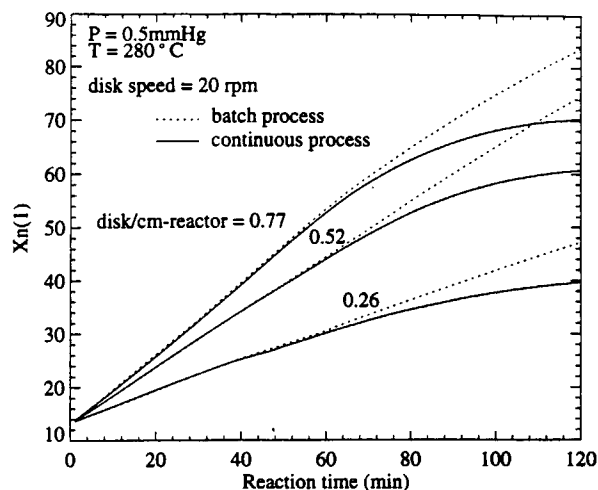**Figure 11**   Effect of disk rotating speed on X_n.

Figure 12 Effect of disk number on X_n.

phase, respectively. Figure 7 shows the fraction of ethylene glycol removed from these two phases. Notice that about 90% of ethylene glycol produced by polycondensation is removed from the film phase formed on the rotating disks. In Figure 8, the fraction of ethylene glycol removed from each disk is shown. Initially, ethylene glycol is removed uniformly from each disk in the reactor. Since the conversion of ethyl hydroxyl groups in the polymer increases most rapidly near the inlet where the concentration of ethyl hydroxyl groups is highest, the fraction of ethylene glycol removed is largest for the disks near the inlet.

Figure 9 shows the scaled amount of ethylene glycol removed from the film phase as well as from the bulk phase as a function of exposure time 30 min after the continuous operation has started. Here the maximum exposure time is 1.8 s (t_f). First, it is seen that the amount of ethylene glycol removed from the bulk phase during this time interval is extremely small, but in the film phase the amount of ethylene glycol removed per revolution is about 10–15% of the initial value.

The effect of mass transfer enhancement factor (f) is shown in Figure 10. If we ignore the contribution of ethylene glycol bubbles to the total mass transfer interfacial area (i.e., $f = 0$), the predicted polymer molecular weight is quite low. In our semibatch polycondensation experiments [2], $f = 1.1$ was used to match the experimental data. This implies that more than half the total interfacial area for ethylene glycol removal is due to ethylene glycol bubbles.

Figure 11 illustrates the effect of disk rotating speed on X_n. The disk rotating speed affects the polymer film thickness on rotating disks and the

film exposure time for mass transfer to vapor phase. Although polymer molecular weight increases somewhat as the disk rotating speed is increased, the effect of disk rotating speed is not quite significant. For high disk rotating speed, the surface renewal time (or film exposure time) is short and the mass transfer coefficient (k_L) increases. On the other hand, the amount of ethylene glycol removed from the film phase per disk rotation becomes small. Thus, the effect of increased mass transfer coefficient is offset to some extent.

The effect of the number of disks on polymer molecular weight is shown in Figure 12. Here dotted lines are for semibatch polycondensation. As more disks are used for a given reactor length, interfacial mass transfer area increases and polymer molecular weight increases accordingly. However, there is a limitation in the number of disks that can be installed for a given reactor size. If there are too many disks, the distance between the disks becomes too small. Then the polymer layers on the adjacent disks stick together, resulting in low specific interfacial area and poor mass transfer efficiency.

CONCLUDING REMARKS

A multicompartment model was proposed for continuous melt polycondensation of poly(ethylene terephthalate) in a rotating disk reactor. In the proposed model, the mass transfer interfacial area on the rotating disks can be determined from the polymer holdup data. An empirical correlation for the film thickness on a rotating disk is used to calculate the specific film phase interfacial area. The effect of ethylene glycol bubbles that provide additional mass transfer interfacial area is accounted for by introducing a mass transfer enhancement factor (f), which is an adjustable model parameter. The model simulation results indicate that most of ethylene glycol formed by polycondensation reaction is removed from the film phase on the rotating disks. As polymer molecular weight increases, the polymer melt viscosity increases, leading to increased polymer holdup on the disk. Thus, the efficiency of ethylene glycol removal from the disks near the outlet of the reactor decreases considerably. It is also possible that if the distance between the disks is too close, the polymer layers on each disk stick together and the available interfacial area decreases significantly. In the proposed multicompartment model, no means are provided to investigate the effect of dead volumes near the outlet of the reactor. Since polymer degradation is likely to occur in such dead

zones where the polymer's residence time is large, it is desirable in future work to modify the reactor model so that such an effect can also be studied. Some issues related to reactor scaleup have not been addressed in this article. For large-scale reactor design, flow patterns should be carefully examined and the viscous heat dissipation effect may have to be considered.

REFERENCES

1. S. I. Cheong and K. Y. Choi, *J. Appl. Polym. Sci.*, **55**, 1819 (1995).
2. S. I. Cheong and K. Y. Choi, *J. Appl. Polym. Sci.*, **58**, 1473 (1995).
3. H. Yokoyama, T. Sano, T. Chijiwa, and R. Kajiya, *Kagaku Kogaku Ronbunshu*, **5**, 236 (1979).
4. K. Ravindranath and R. A. Mashelkar, *Polym. Eng. Sci.*, **22**, 628 (1982).
5. K. Ravindranath and R. A. Mashelkar, *A.I.Ch. E. J.*, **30**, 415 (1984).
6. A. Kumar, S. K. Gupta, A. Ghosh, and S. K. Gupta, *J. Appl. Polym. Sci.*, **29**, 3217 (1984).
7. A. Kumar, S. K. Gupta, S. Madan, N. G. Shah, and S. K. Gupta, *Polym. Eng. Sci.*, **24**, 194 (1984).
8. C. Laubriet, B. LeCorre, and K. Y. Choi, *Ind. & Eng. Chem. Res.*, **29**, 2 (1991).
9. H. Castres Saint Martin and K. Y. Choi, *Ind. & Eng. Chem. Res.*, **30**, 1712 (1991).
10. M. Amon and C. D. Denson, *Ind. & Eng. Chem. Fundam.*, **19**, 415 (1980).
11. T. M. Pell, Jr., and T. G. Davis, *J. Polym. Sci.: Polym. Phys.*, **11**, 1671 (1973).
12. G. D. Lei and K. Y. Choi, *J. Appl. Polym. Sci.*, **41**, 2987 (1990).